

**NASA TECHNICAL  
MEMORANDUM**



*N73-25998*  
NASA TM X-2786

NASA TM X-2786

**CASE FILE  
COPY**

**SUBSONIC AERODYNAMIC CHARACTERISTICS  
OF A SPACE SHUTTLE ORBITER**

*by James C. Ellison*

*Langley Research Center*

*Hampton, Va. 23665*

1. Report No. NASA TM X-2786	2. Government Accession No.	3. Recipient's Catalog No.	
4. Title and Subtitle SUBSONIC AERODYNAMIC CHARACTERISTICS OF A SPACE SHUTTLE ORBITER		5. Report Date July 1973	
		6. Performing Organization Code	
7. Author(s) James C. Ellison		8. Performing Organization Report No. L-8765	
9. Performing Organization Name and Address NASA Langley Research Center Hampton, Va. 23665		10. Work Unit No. 502-37-01-01	
		11. Contract or Grant No.	
12. Sponsoring Agency Name and Address National Aeronautics and Space Administration Washington, D.C. 20546		13. Type of Report and Period Covered Technical Memorandum	
		14. Sponsoring Agency Code	
15. Supplementary Notes			
16. Abstract  <p>An investigation of a space shuttle orbiter has been conducted in the Langley low-turbulence pressure tunnel at a Mach number of 0.25 and Reynolds numbers from <math>4.17 \times 10^6</math> to <math>29.17 \times 10^6</math>, based on model length. The angle-of-attack range was about <math>-4^\circ</math> to <math>24^\circ</math> at angles of sideslip of <math>0^\circ</math> and <math>5^\circ</math>. Static longitudinal and lateral-directional aerodynamic characteristics were obtained for elevon deflections from <math>0^\circ</math> to <math>-20^\circ</math>.</p> <p>The model was longitudinally stable at all test conditions; however, depending on Reynolds number and elevon-deflection angle, the model was directionally unstable for angles of attack between <math>9^\circ</math> and <math>17^\circ</math>. The model had a maximum trimmed lift-drag ratio of about 6.25 which occurred at an angle of attack of about <math>9^\circ</math> with an elevon deflection of <math>-10^\circ</math>.</p>			
17. Key Words (Suggested by Author(s))  Shuttle orbiter Aerodynamic characteristics		18. Distribution Statement  Unclassified - Unlimited	
19. Security Classif. (of this report) Unclassified	20. Security Classif. (of this page) Unclassified	21. No. of Pages 24	22. Price* \$3.00

**Page Intentionally Left Blank**

# SUBSONIC AERODYNAMIC CHARACTERISTICS OF A SPACE SHUTTLE ORBITER

By James C. Ellison  
Langley Research Center

## SUMMARY

Low-subsonic wind-tunnel tests have been conducted to determine the static longitudinal and lateral-directional aerodynamic characteristics of a space shuttle orbiter. Data were obtained at angles of attack from about  $-4^{\circ}$  to  $24^{\circ}$  at angles of sideslip of  $0^{\circ}$  and  $5^{\circ}$  for Reynolds numbers ranging from  $4.17 \times 10^6$  to  $29.17 \times 10^6$ , based on model length. Elevon effectiveness was investigated by setting the elevons at deflection angles of  $0^{\circ}$ ,  $-10^{\circ}$ ,  $-15^{\circ}$ , and  $-20^{\circ}$ .

Increasing Reynolds number from  $4.17 \times 10^6$  to  $29.17 \times 10^6$  had essentially no effect on the longitudinal characteristics but had significant effects on the lateral-directional characteristics. The model was longitudinally stable about the test center-of-gravity position of 0.67 body length at all angles of attack and elevon deflections tested. The maximum trimmed lift-drag ratio of about 6.25 was obtained at an angle of attack of about  $9^{\circ}$  with an elevon deflection of  $-10^{\circ}$  with significant trim penalties at other elevon-deflection angles. Depending on Reynolds number and elevon deflection, the model was directionally unstable at angles of attack between  $9^{\circ}$  and  $17^{\circ}$ .

## INTRODUCTION

The National Aeronautics and Space Administration and the aerospace industry are presently investigating, experimentally and analytically, configurations suitable for transporting large payloads to and from near-earth orbit. (See refs. 1 to 3.) The basic concept incorporates a reusable orbiter which is vertically launched, separates from the booster system at some point in the flight, and is capable of aircraft-type horizontal landing following reentry. This paper presents the results of an investigation of the subsonic aerodynamic characteristics of an orbiter concept designed for use in a fully reusable, two-stage, shuttle system.

The study examined the effects of Reynolds number on the static longitudinal and lateral-directional stability characteristics and the effectiveness of the elevons as longitudinal controls. The investigation was conducted in the Langley low-turbulence



pressure tunnel at a Mach number of 0.25 for angles of attack from  $-4^\circ$  to  $24^\circ$  at sideslip angles of  $0^\circ$  and  $5^\circ$  over a range of Reynolds numbers from  $4.17 \times 10^6$  to  $29.17 \times 10^6$ , based on model length.

## SYMBOLS

The static longitudinal characteristics are referred to the stability axes, and the lateral-directional characteristics are referred to the body axes. All coefficients are normalized with respect to the theoretical wing planform area, the mean aerodynamic wing chord, and the wing span. The moment reference point corresponds to a center-of-gravity location at 67 percent of the body length and 41 percent of the body height at this longitudinal station.

$b$  wing span

$C_D$  drag coefficient,  $\frac{\text{Drag}}{q_\infty S}$

$C_L$  lift coefficient,  $\frac{\text{Lift}}{q_\infty S}$

$C_l$  rolling-moment coefficient,  $\frac{\text{Rolling moment}}{q_\infty S b}$

$C_{l_\beta}$  lateral-stability parameter,  $\Delta C_l / \Delta \beta$ , where  $\beta = 0^\circ$  and  $5^\circ$

$C_m$  pitching-moment coefficient,  $\frac{\text{Pitching moment}}{q_\infty S \bar{c}}$

$C_{m,0}$  pitching-moment coefficient at  $C_L = 0$

$C_n$  yawing-moment coefficient,  $\frac{\text{Yawing moment}}{q_\infty S b}$

$C_{n_\beta}$  directional-stability parameter,  $\Delta C_n / \Delta \beta$ , where  $\beta = 0^\circ$  and  $5^\circ$

$C_{n_\beta, \text{dyn}} = C_{n_\beta} \cos \alpha - (I_Z / I_X) C_{l_\beta} \sin \alpha$

$C_{p,b}$  base-pressure coefficient,  $\frac{p_b - p_\infty}{q_\infty}$

$C_Y$  side-force coefficient,  $\frac{\text{Side force}}{q_\infty S}$

$C_{Y\beta}$	side-force parameter, $\Delta C_Y/\Delta\beta$ , where $\beta = 0^\circ$ and $5^\circ$
$\bar{c}$	mean aerodynamic chord
$I_X$	moment of inertia about longitudinal body axis, kilogram-meters <sup>2</sup> (slug-feet <sup>2</sup> )
$I_Z$	moment of inertia about normal body axis, kilogram-meters <sup>2</sup> (slug-feet <sup>2</sup> )
$i_w$	wing incidence angle
$L/D$	lift-drag ratio
$(L/D)_{\max}$	maximum lift-drag ratio
$l$	length of body
$p_b$	base pressure
$p_\infty$	free-stream static pressure
$q_\infty$	free-stream dynamic pressure
$R$	Reynolds number based on body length
$S$	theoretical wing planform area
$S_b$	base area
$S_t$	vertical-tail planform area
$y$	spanwise coordinate (see fig. 1)
$\alpha$	angle of attack, deg
$\beta$	angle of sideslip, deg
$\Delta( )$	incremental values
$\delta_e$	elevon-deflection angle, positive when trailing edge down

## DESCRIPTION OF MODEL

A sketch of the model is presented in figure 1 and photographs of the model are shown in figure 2. The basic configuration consisted of a blended delta wing-body with a center-line vertical tail. The wing (NACA 0010-64 at the root and NACA 0012-64 at the tip) had  $2^\circ$  of incidence and  $10^\circ$  of dihedral with full-span elevons which could be set at deflection angles of  $0^\circ$ ,  $-10^\circ$ ,  $-15^\circ$ , and  $-20^\circ$ . Provisions were made to test the model with and without the vertical tail.

## TESTS AND CORRECTIONS

The tests were conducted in the Langley low-turbulence pressure tunnel (ref. 4) by using a smooth model at a Mach number of 0.25 over a range of Reynolds numbers from  $4.17 \times 10^6$  to  $29.17 \times 10^6$ , based on model length. Forces and moments were measured with a sting-supported, six-component, strain-gage balance. The angle of attack was varied from about  $-4^\circ$  to  $24^\circ$  at angles of sideslip of  $0^\circ$  and  $5^\circ$ .

Angles of attack and sideslip have been corrected for the effects of sting and balance deflections due to aerodynamic loads. The data have been corrected for wind-tunnel blockage. The drag coefficients represent gross drag in that no correction was made for base pressure; however, the base-pressure coefficient, an average of two measurements, has been presented.

## RESULTS AND DISCUSSION

The results of this investigation are presented as longitudinal and lateral-directional aerodynamic characteristics in figures 3 to 5 and figures 6 to 9, respectively.

### Longitudinal Aerodynamic Characteristics

Effect of Reynolds number. - The longitudinal aerodynamic characteristics of the model with the elevons deflected  $-10^\circ$  (which most nearly represents the condition of maximum trimmed  $L/D$ ) are shown in figure 3. As can be seen in figures 3(b) and 3(c) no consistent trend in the variation of drag coefficient or  $(L/D)_{\max}$  with Reynolds number is apparent. The values of  $C_D$  for a given value of  $C_L$  remained essentially constant for Reynolds numbers of  $20.83 \times 10^6$  and above; hence, the remaining longitudinal data are presented for  $R = 20.83 \times 10^6$ .

Effect of elevon deflection. - The longitudinal characteristics of the model with various elevon-deflection angles are presented in figure 4; these data were utilized to obtain the trim characteristics in figure 5. The model was statically stable throughout the angle-of-attack range (center of gravity at 0.67) for all elevon-deflection angles tested,

and deflection of the elevons produced a nearly linear variation in pitching moment. A large negative out-of-trim pitching moment exists at  $\alpha = 0^\circ$  and  $\delta_e = 0^\circ$ , as indicated by the circular symbols in figure 4(c). The wing incidence of  $2^\circ$  produced a negative  $C_{m,o}$ , but the value of  $C_{m,o}$  attributable to the theoretical wing planform was calculated as -0.016 (ref. 5), much less than the measured value of -0.061 for the complete model. The major portion of the out-of-trim moment is probably caused by the drooped body nose and the fairing of the wing-to-body contours. An examination of the chordwise mean-line distribution of two inboard wing sections (where the wing-to-body fairing covers the original theoretical airfoil section) showed that the root-station ( $y/b = 0.265$ ) mean-line camber was about 1.9 percent chord, and the station at  $y/b = 0.369$  mean-line camber was about 0.9 percent chord. (See fig. 1.) Reference 5 indicates that airfoil sections with about 2.0 percent mean-line camber produce a value of  $C_{m,o}$  of -0.05, based on the local chord. Although the out-of-trim moments produced by the cambered inboard sections of the model wing would have to be weighted to obtain a reasonable estimate of their contribution, it is obvious that they have a major influence on the total model out-of-trim moment. The trim data (fig. 5) indicate that an elevon-deflection angle of  $-6.75^\circ$  is required to trim out the negative  $C_{m,o}$ , and an elevon-deflection angle of  $-14^\circ$  is required to trim the model at the landing attitude ( $\alpha = 17^\circ$ ). This large deflection of the elevons for trim reduces the value of  $C_L$  at  $\alpha = 17^\circ$  from 0.84 to 0.58. The lift-drag ratio had a maximum untrimmed value of about 7.0. The maximum trimmed lift-drag ratio of about 6.25 was obtained at  $\alpha \approx 9^\circ$  with  $\delta_e = -10^\circ$  with significant trim penalties at other elevon-deflection angles.

#### Lateral-Directional Aerodynamic Characteristics

The lateral-directional parameters  $C_{l_\beta}$ ,  $C_{n_\beta}$ , and  $C_{Y_\beta}$  were calculated from the increments in  $C_l$ ,  $C_n$ , and  $C_Y$ , respectively, between  $\beta = 0^\circ$  and  $5^\circ$ ; therefore, they do not account for any nonlinearities which may exist in the intermediate sideslip range.

Effect of Reynolds number.— The results presented in figure 6 indicate an increase in directional stability with increases in Reynolds number over the angle-of-attack range; however, between  $\alpha = 9^\circ$  and  $17^\circ$ , depending on Reynolds number, there was an unstable region followed by a stable region at the higher angles of attack. The magnitude of the loss in directional stability was reduced and the rate of recovery was increased as the Reynolds number increased, but increasing Reynolds number did not eliminate the unstable region. For  $\alpha > 12^\circ$  the positive effective dihedral ( $-C_{l_\beta}$ ) decreased as the Reynolds number was increased, and it appeared to correspond with the recovery in directional stability noted previously.

Visual-flow observations using tufts attached to the model indicated bound vortices originating at the leading edge of the wing and at the wing-body juncture which increased in intensity with angle of attack. When the model was yawed, the vortices on the windward side shifted inboard and the wing-body-juncture vortex swept the body side with high-energy flow. As angle of attack increased, the high-energy flow from the vortex apparently generated negative pressures on the body side rearward of the moment center of sufficient magnitude to reduce the directional stability, especially at the lower Reynolds number where the influence of vortices is relatively stronger.

The continued increase in positive effective dihedral with increasing angle of attack at the low Reynolds numbers suggests that the vortex influence over the windward wing is strong enough to maintain unseparated flow over the wing tip up to  $\alpha \approx 17^\circ$ . The relative strength of the bound vortices decreased with increasing Reynolds number, thus reducing the influence on the aerodynamic loading over the upper wing and body side surfaces rearward of the center of gravity. Furthermore, at the higher Reynolds number this probable reduction of the negative pressure distribution on the windward portion of the rear body coupled with the earlier separation of the outboard portion of the windward wing resulted in increased directional stability and reduced effective dihedral. Similar effects of leading-edge bound vortices on the lateral-directional characteristics of highly swept wings have been presented in reference 6, and the effect of Reynolds number on vortex flow has been shown in reference 7.

Effect of elevon deflection. - The effect of elevon deflections on the lateral-directional stability is shown in figure 7 for  $R = 20.83 \times 10^6$ . In the range about  $9^\circ < \alpha < 13^\circ$  the configuration was directionally unstable for  $\delta_e = 0^\circ$ ,  $-10^\circ$ , and  $-15^\circ$  with the greatest instability resulting for  $\delta_e = 0^\circ$ . Above  $\alpha = 13^\circ$  the directional stability was regained at all elevon-deflection angles investigated with the greatest recovery being achieved with  $\delta_e = 0^\circ$  and  $-10^\circ$ ; however, at about  $\alpha = 19.5^\circ$  the configuration with  $\delta_e = -20^\circ$  became unstable. For  $\alpha < 12^\circ$  the positive effective dihedral increased when the elevon-deflection angle was changed from  $0^\circ$  to  $-10^\circ$ , but the effect of elevons on  $C_{l_\beta}$  reversed as the elevons were deflected to greater negative angles for angles of attack below about  $16^\circ$ . The effective dihedral, for all elevon-deflection angles tested, decreased above  $\alpha = 11^\circ$  as the angle of attack increased. Although the model lost static directional stability at some angles of attack for all elevon-deflection angles, figure 8 shows that the model retained dynamic directional stability ( $C_{n_{\beta, \text{dyn}}}$ ) at all angles of attack for the longitudinally trimmed case.

Effect of vertical tail. - The effect of the vertical tail on the lateral-directional aerodynamic characteristics for  $\delta_e = 0^\circ$  is shown in figure 9. As can be seen from this figure, the vertical tail produced a nearly constant increment in directional stability, and the large decrease in  $C_{n_\beta}$  between  $\alpha \approx 8^\circ$  and  $14^\circ$  was not affected by its presence.

This indicates that the loading on the vertical tail was not influenced by the vortex-type flow in the wing-body juncture. The positive effective dihedral was significantly decreased when the vertical tail was removed. Near  $\alpha = 11^\circ$  the value of  $C_{l_\beta}$  began to increase and became positive at  $\alpha = 16^\circ$  with the vertical tail and at  $\alpha = 14^\circ$  without the vertical tail.

## SUMMARY OF RESULTS

Low-subsonic wind-tunnel tests have been conducted to determine the static longitudinal and lateral-directional aerodynamic characteristics of a space shuttle orbiter. The results of the investigation are summarized as follows:

1. Increasing the Reynolds number from  $4.17 \times 10^6$  to  $29.17 \times 10^6$  had essentially no effect on the longitudinal characteristics, but it had significant effects on the lateral-directional characteristics.
2. The model was longitudinally stable about the test center-of-gravity position of 0.67 body length for all angles of attack and elevon-deflection angles tested.
3. The maximum trimmed lift-drag ratio of about 6.25 was obtained at an angle of attack of about  $9^\circ$  with an elevon deflection of  $-10^\circ$  with significant trim penalties at other elevon-deflection angles.
4. Depending on Reynolds number and elevon-deflection angle, the model was directionally unstable at angles of attack between  $9^\circ$  and  $17^\circ$ .

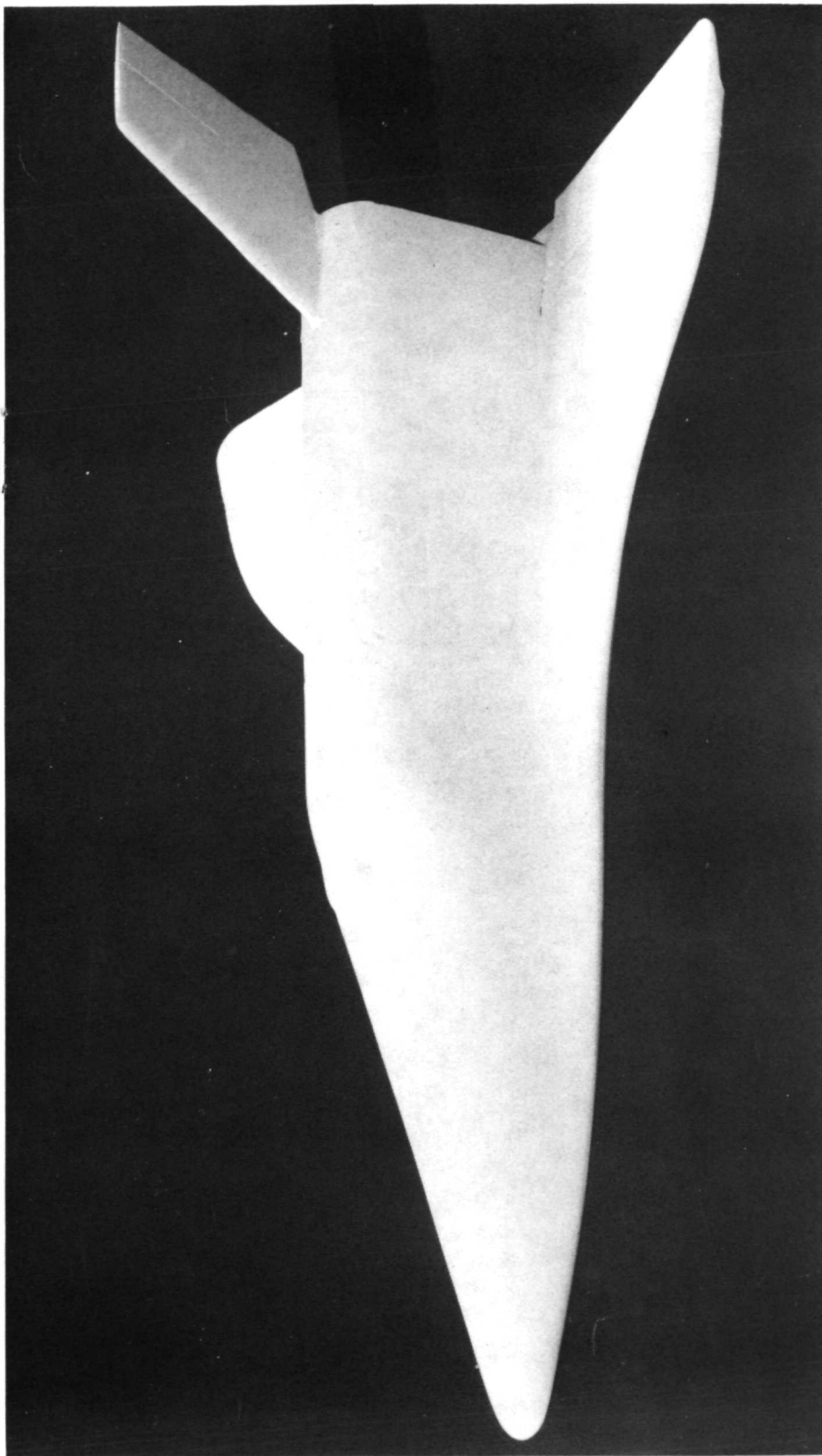
Langley Research Center,  
National Aeronautics and Space Administration,  
Hampton, Va., May 9, 1973.

## REFERENCES

1. Ware, George M.; and Spencer, Bernard, Jr.: Low-Subsonic Aerodynamic Characteristics of a Shuttle-Orbiter Configuration With a Variable-Dihedral Delta Wing. NASA TM X-2206, 1971.
2. Freeman, Delma C., Jr.: Low-Subsonic Aerodynamic Characteristics of a Space Shuttle-Orbiter Concept With a Blended Delta Wing-Body. NASA TM X-2209, 1971.
3. Fox, Charles H., Jr.; and Freeman, Delma C., Jr.: Subsonic Stability, Control, and Performance of a Shuttle Concept With a Blended Wing-Body. NASA TM X-2341, 1971.
4. Pirrello, C. J.; Hardin, R. D.; Heckart, M. V.; and Brown, K. R.: An Inventory of Aeronautical Ground Research Facilities. Vol. I - Wind Tunnels. NASA CR-1874, 1971.
5. Abbott, Ira H.; and Von Doenhoff, Albert E.: Theory of Wing Sections. Dover Publ., Inc., c.1959.
6. Lovell, J. Calvin; and Wilson, Herbert A., Jr.: Langley Full-Scale Tunnel Investigation of Maximum Lift and Stability Characteristics of an Airplane Having Approximately Triangular Plan Form (DM-1 Glider). NACA RM L7F16, 1947.
7. Wilson, Herbert A., Jr.; and Lovell, J. Calvin: Full-Scale Investigation of the Maximum Lift and Flow Characteristics of an Airplane Having Approximately Triangular Plan Form. NACA RM L6K20, 1947.



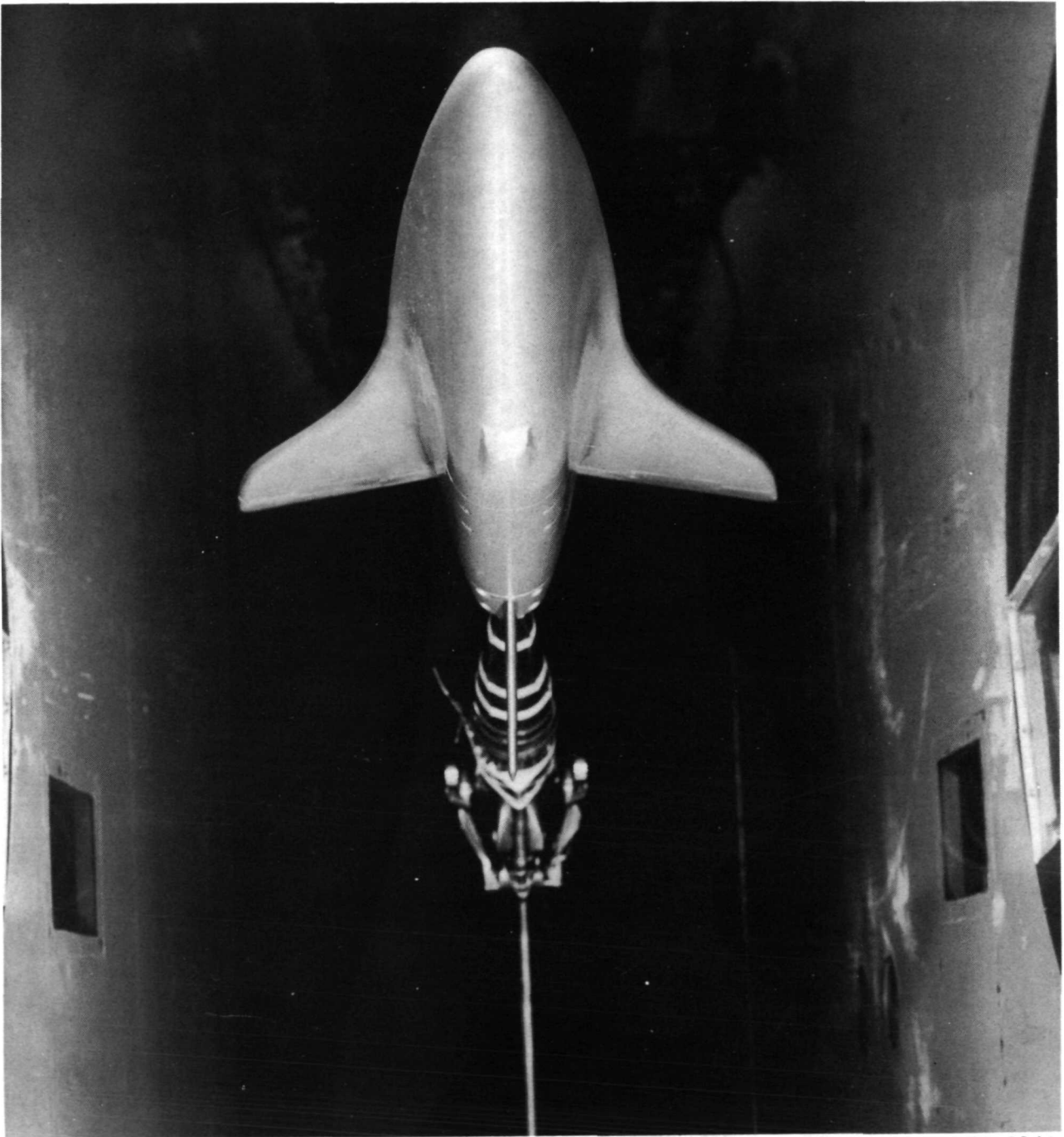




L-71-4059

(a) Side view.

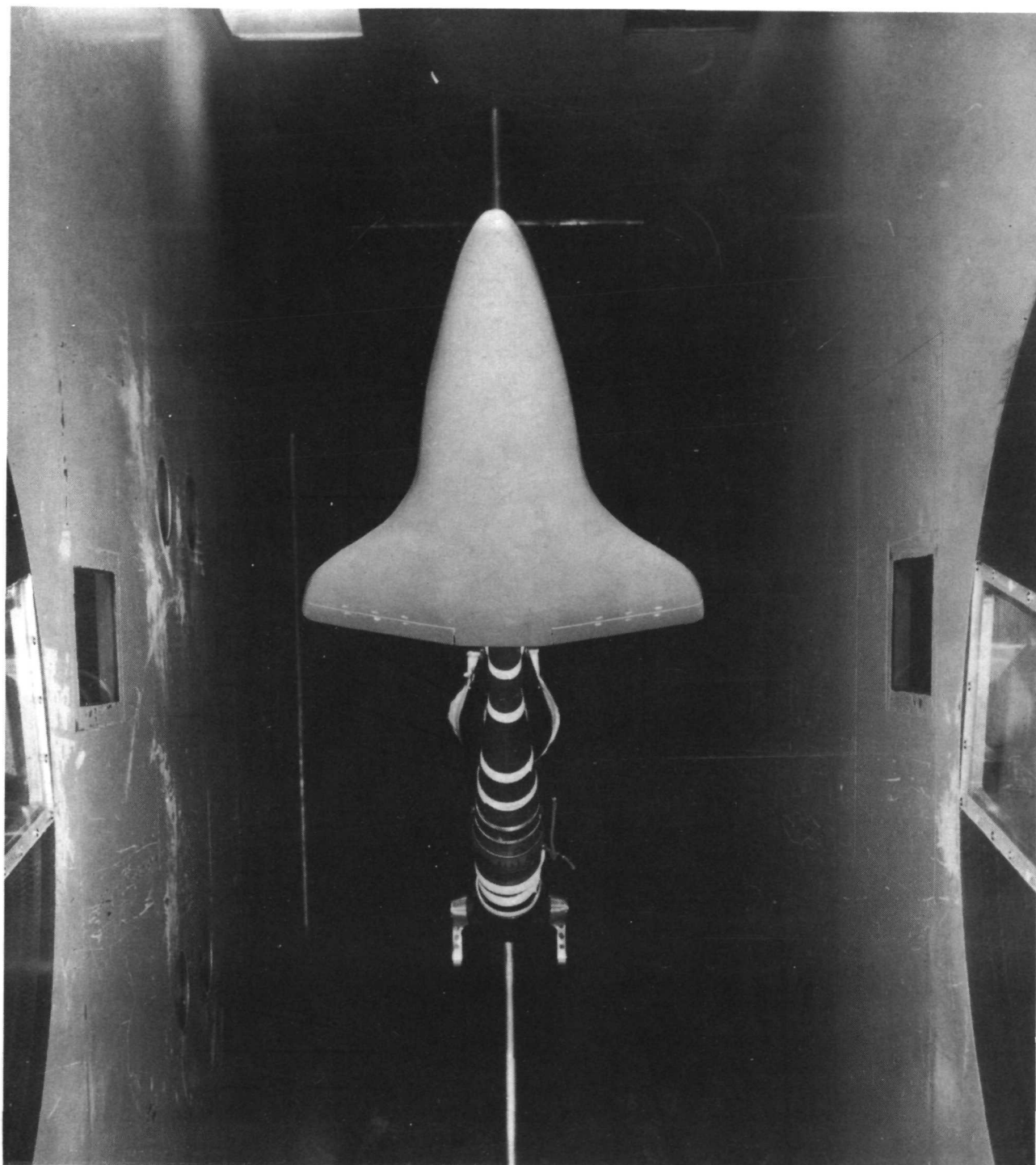
Figure 2.- Photographs of the model.



L-71-3840

(b) Top view.

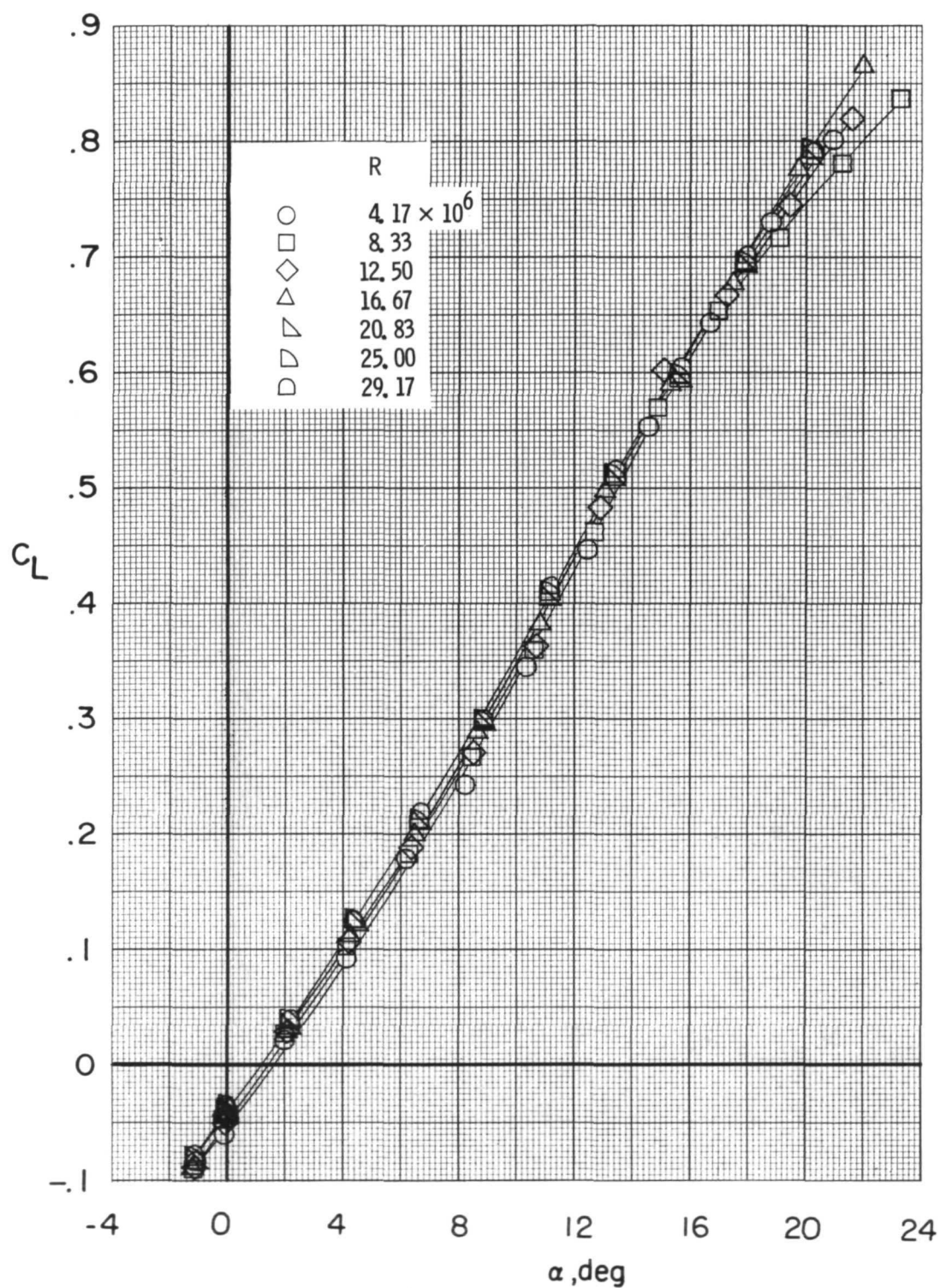
Figure 2.- Continued.



L-71-3841

(c) Bottom view.

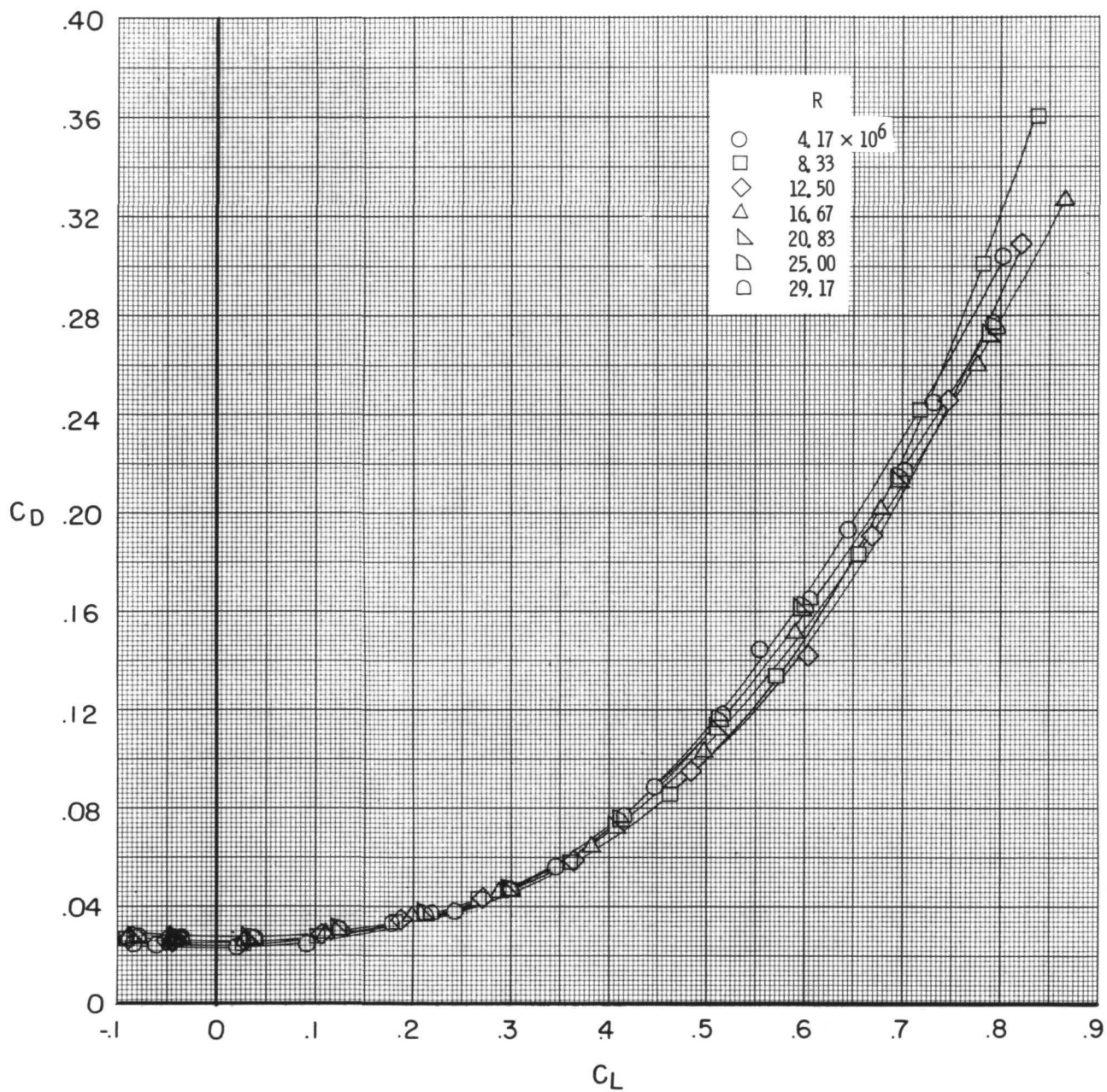
Figure 2.- Concluded.



(a)  $C_L$  as a function of  $\alpha$ .

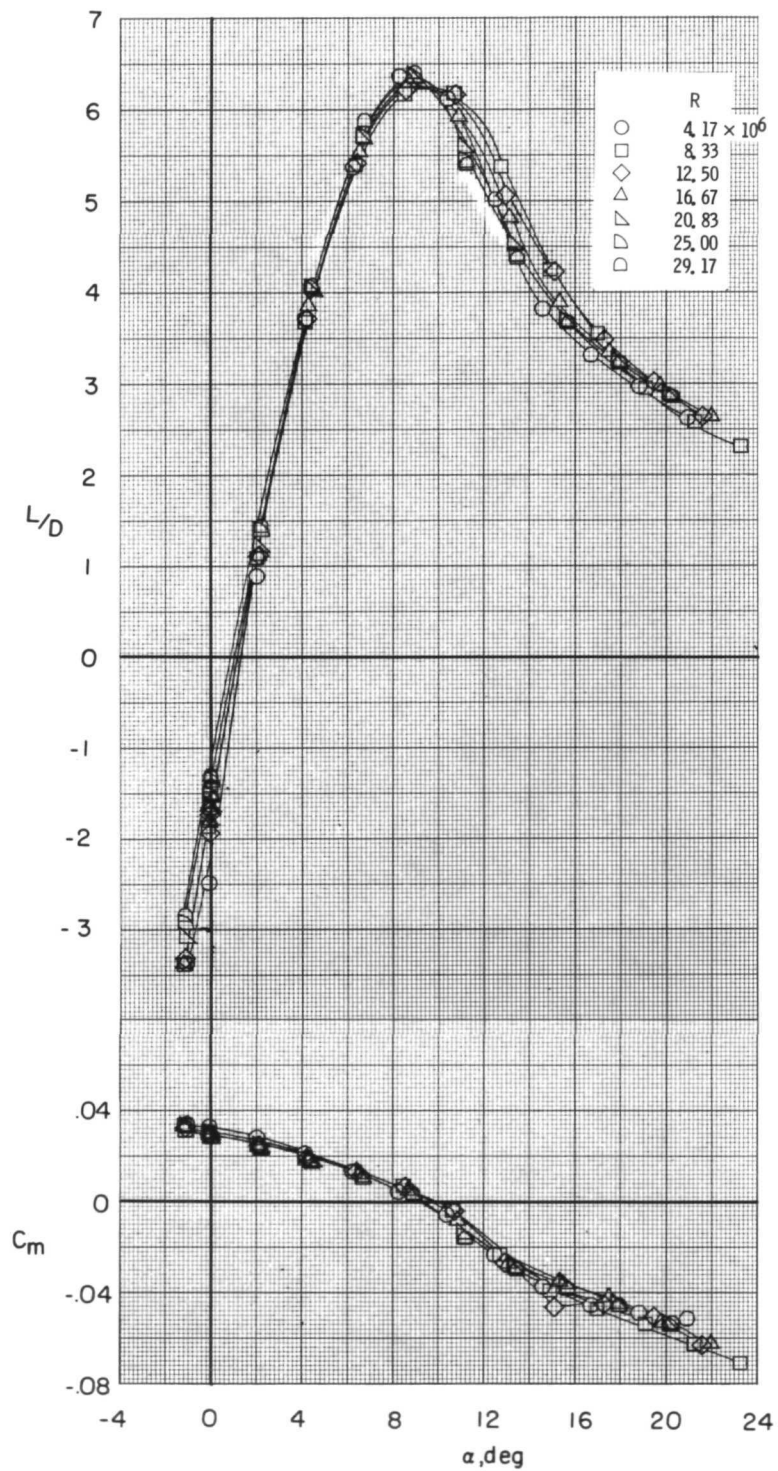
Figure 3.- Effect of Reynolds number on the longitudinal aerodynamic characteristics.  $\delta_e = -10^\circ$ .





(b)  $C_D$  as a function of  $C_L$ .

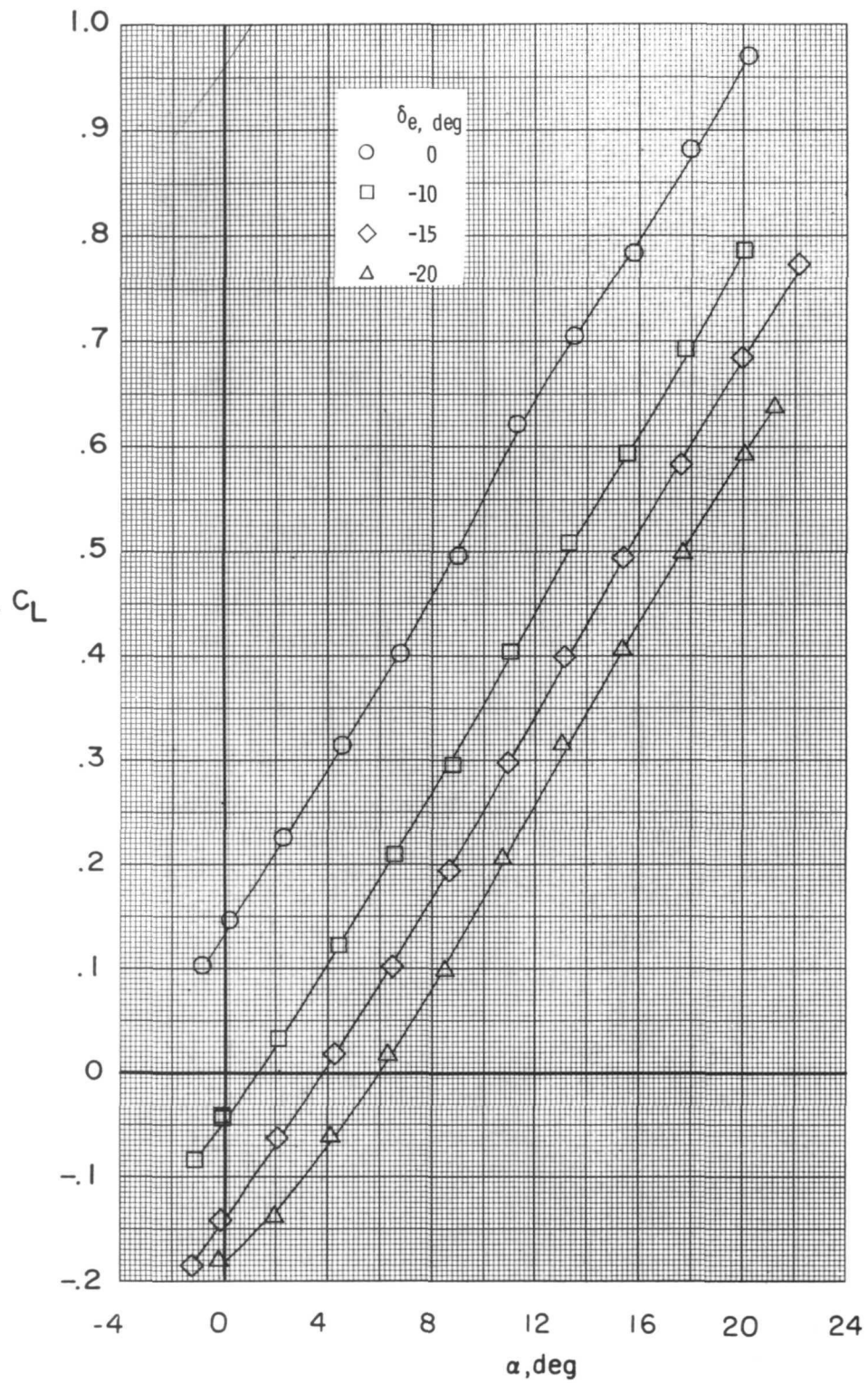
Figure 3.- Continued.



(c)  $L/D$  and  $C_m$  as a function of  $\alpha$ .

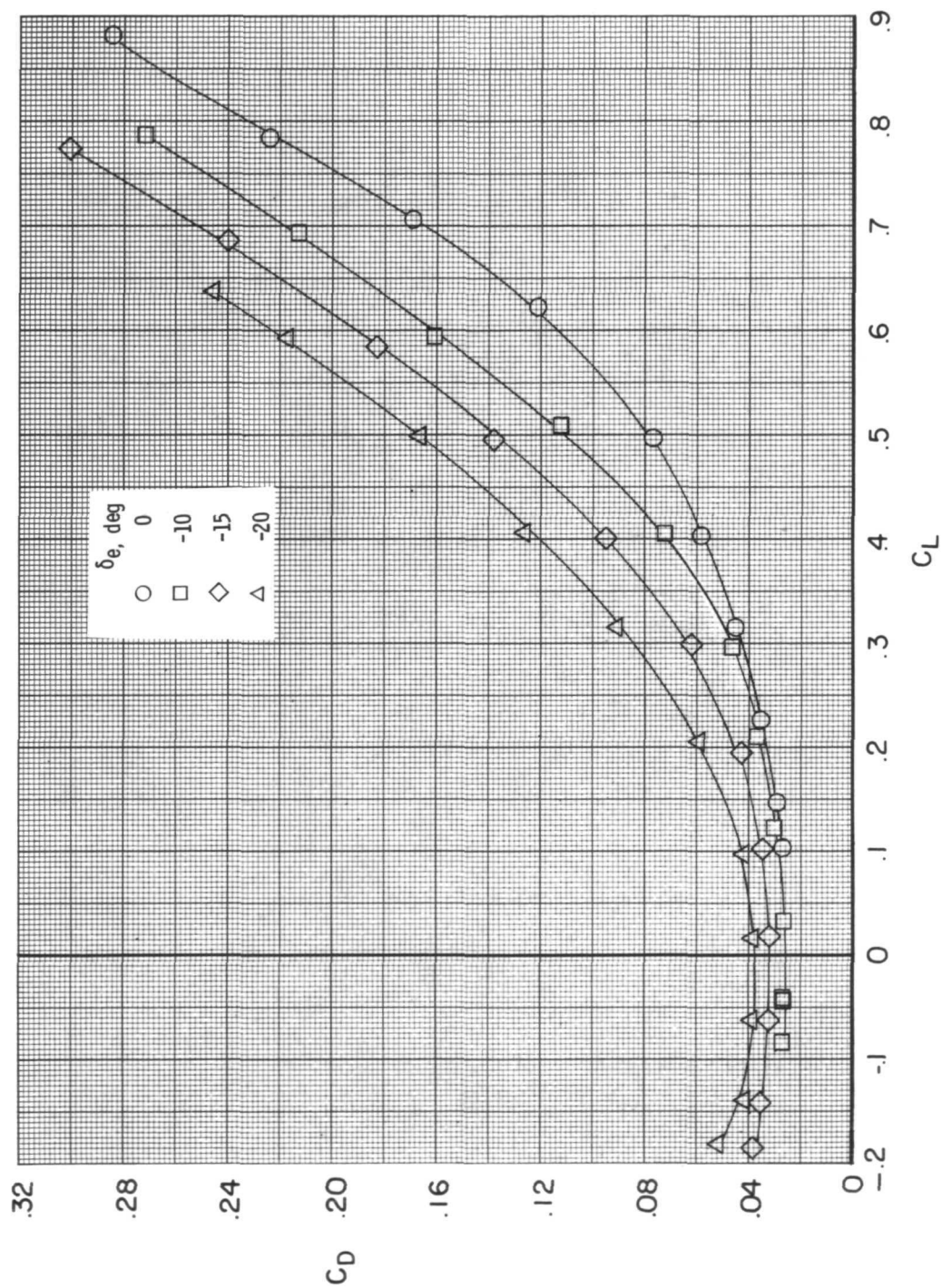
Figure 3.- Concluded.





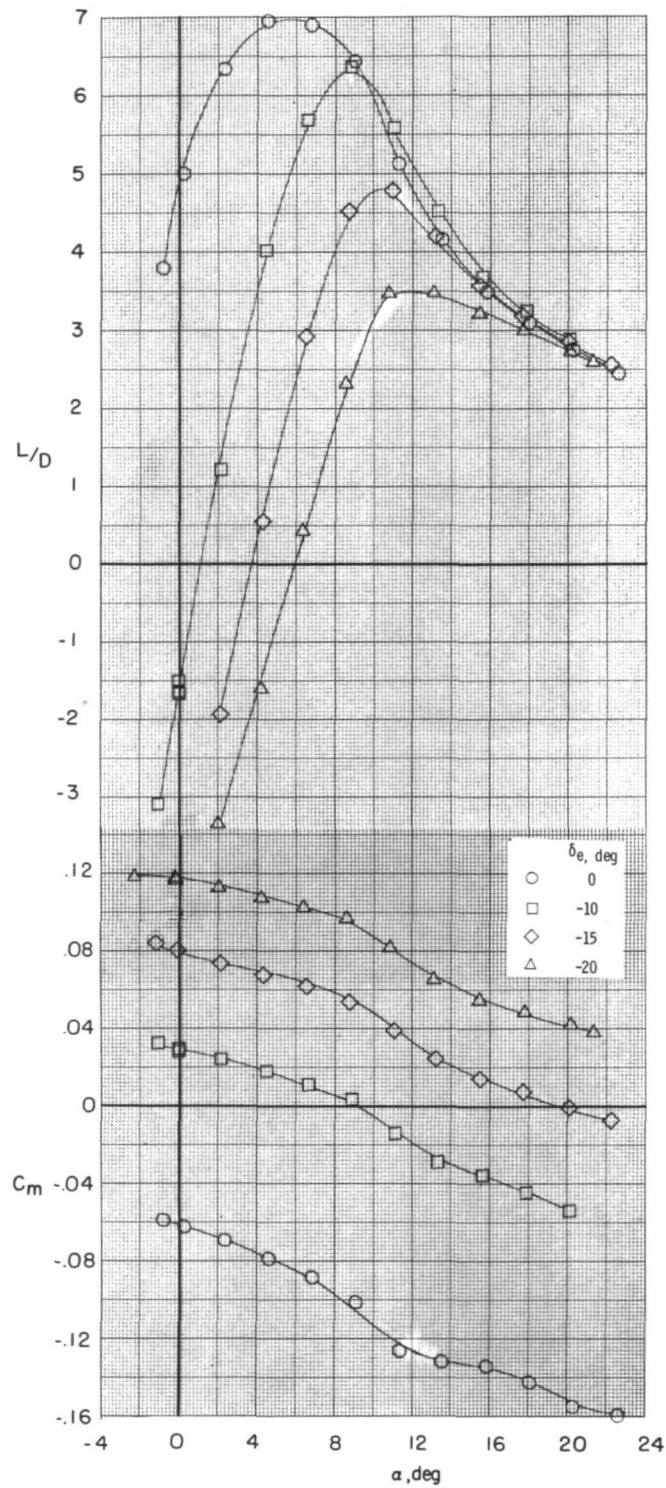
(a)  $C_L$  as a function of  $\alpha$ .

Figure 4.- Effect of elevon deflection on the longitudinal aerodynamic characteristics.  $R = 20.83 \times 10^6$ .



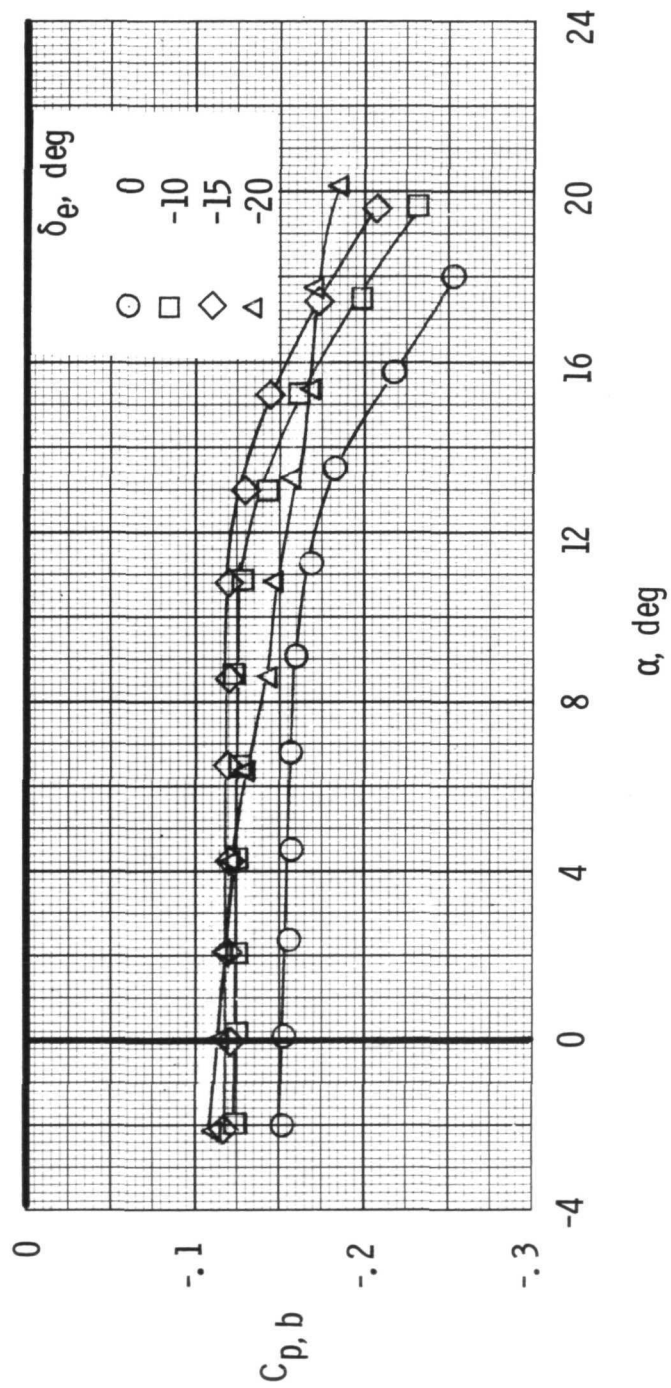
(b)  $C_D$  as a function of  $C_L$ .

Figure 4.- Continued.



(c)  $L/D$  and  $C_m$  as a function of  $\alpha$ .

Figure 4.- Continued.



(d) Average base-pressure coefficient.  $S_b = 73.68 \text{ cm}^2$ .

Figure 4.- Concluded.

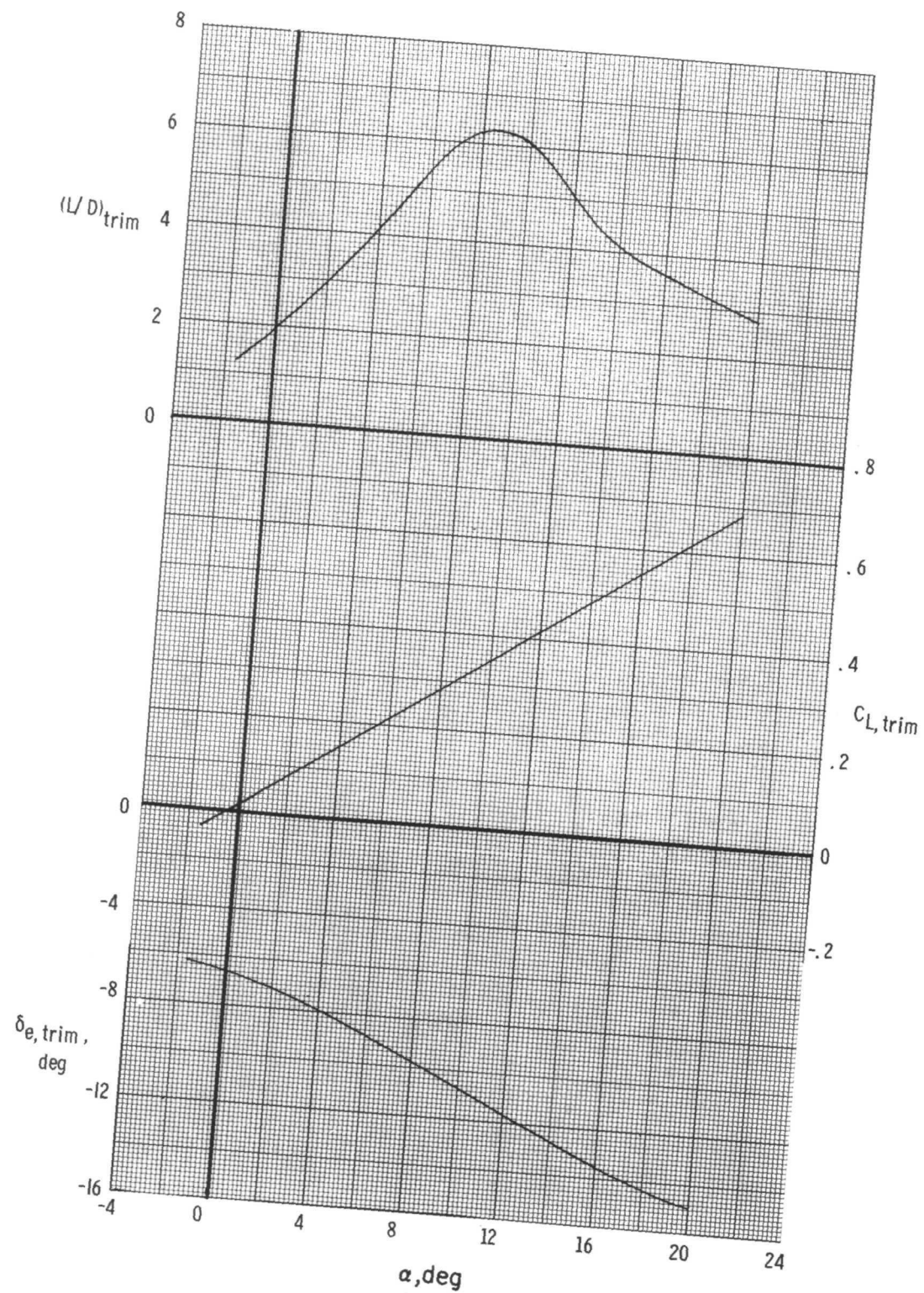


Figure 5.- Trim characteristics.  $R = 20.83 \times 10^6$ .



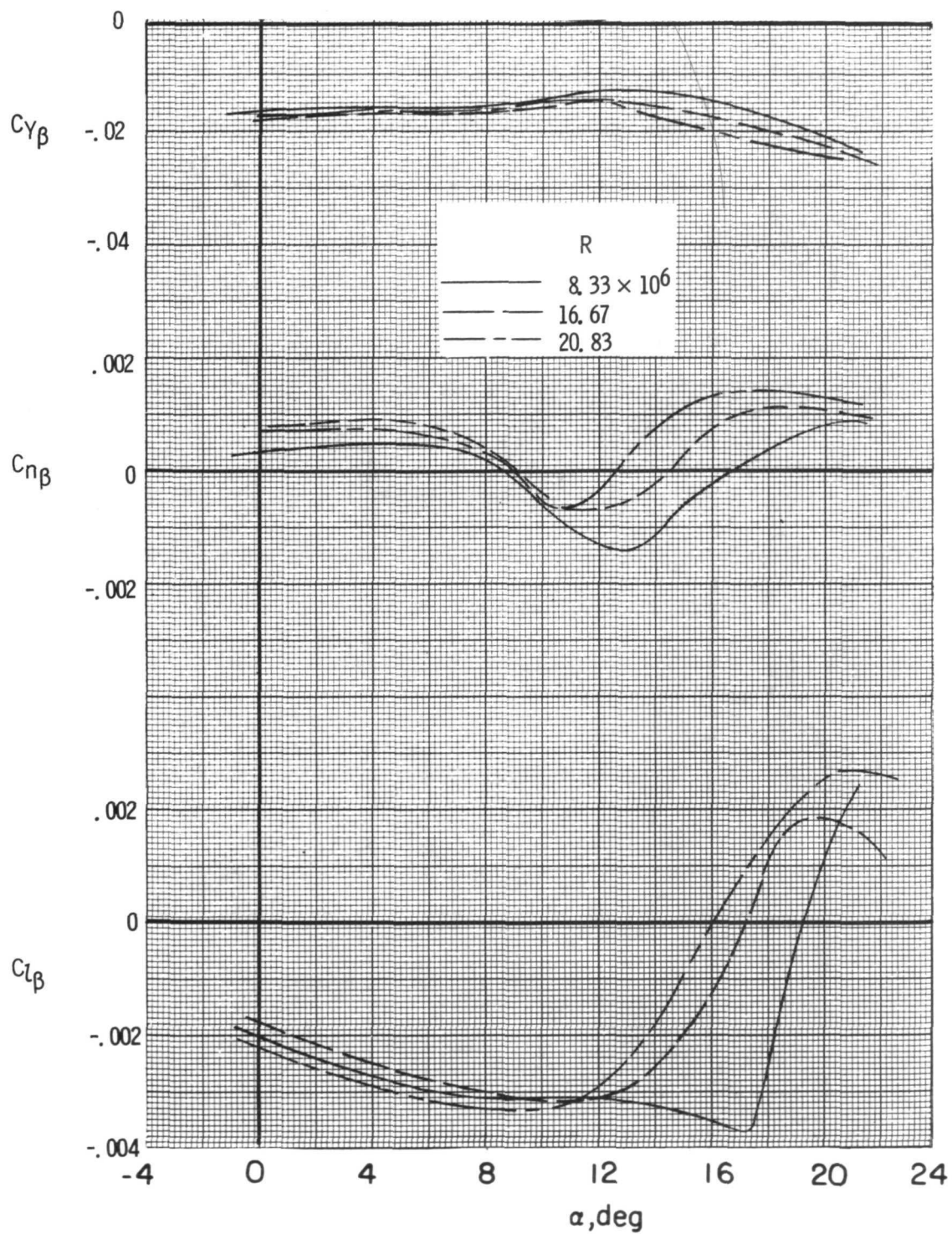


Figure 6.- Effect of Reynolds number on the lateral-directional stability derivatives.  $\delta_e = 0^\circ$ .

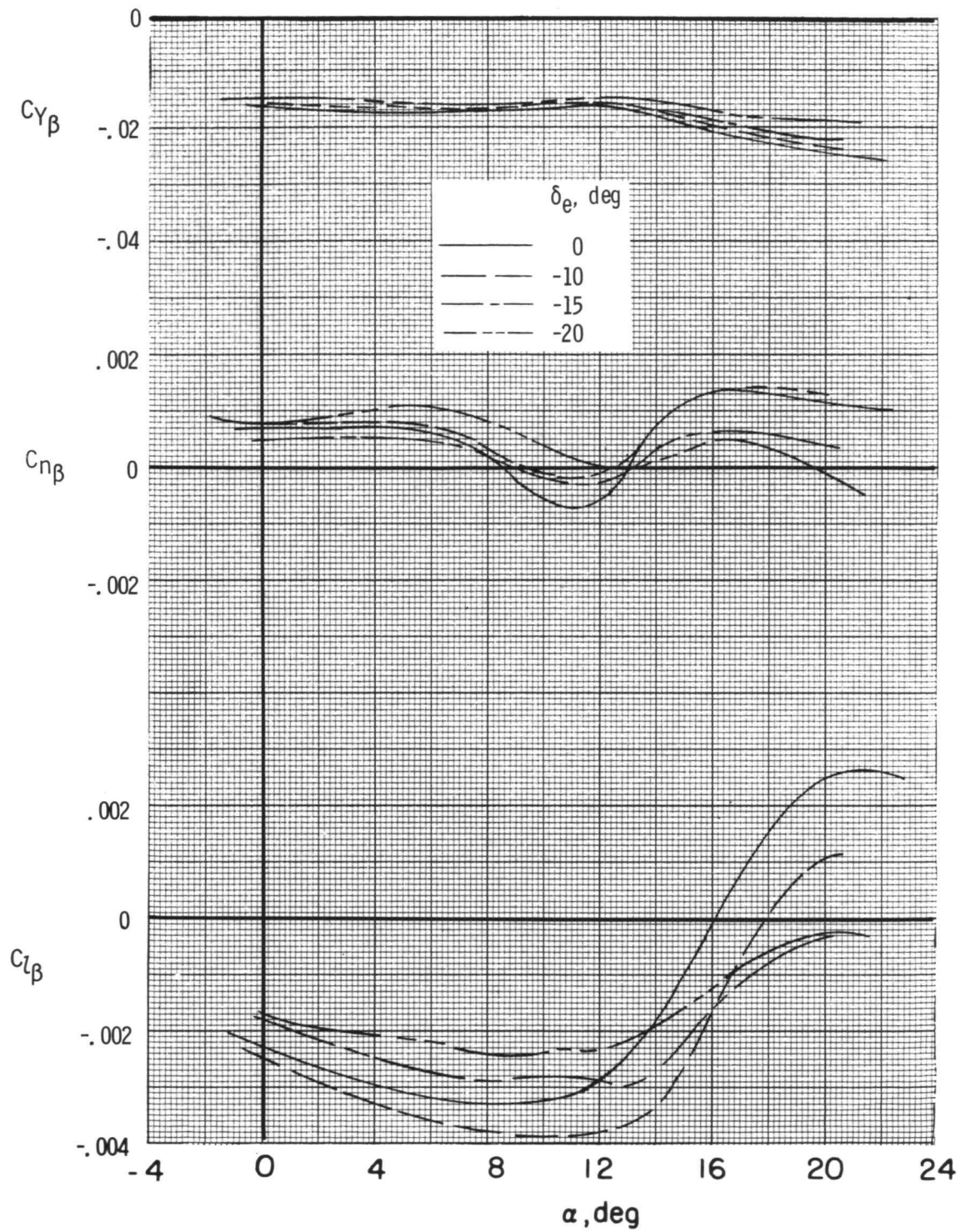


Figure 7.- Effect of elevon deflection on the lateral-directional stability derivatives.  $R = 20.83 \times 10^6$ .



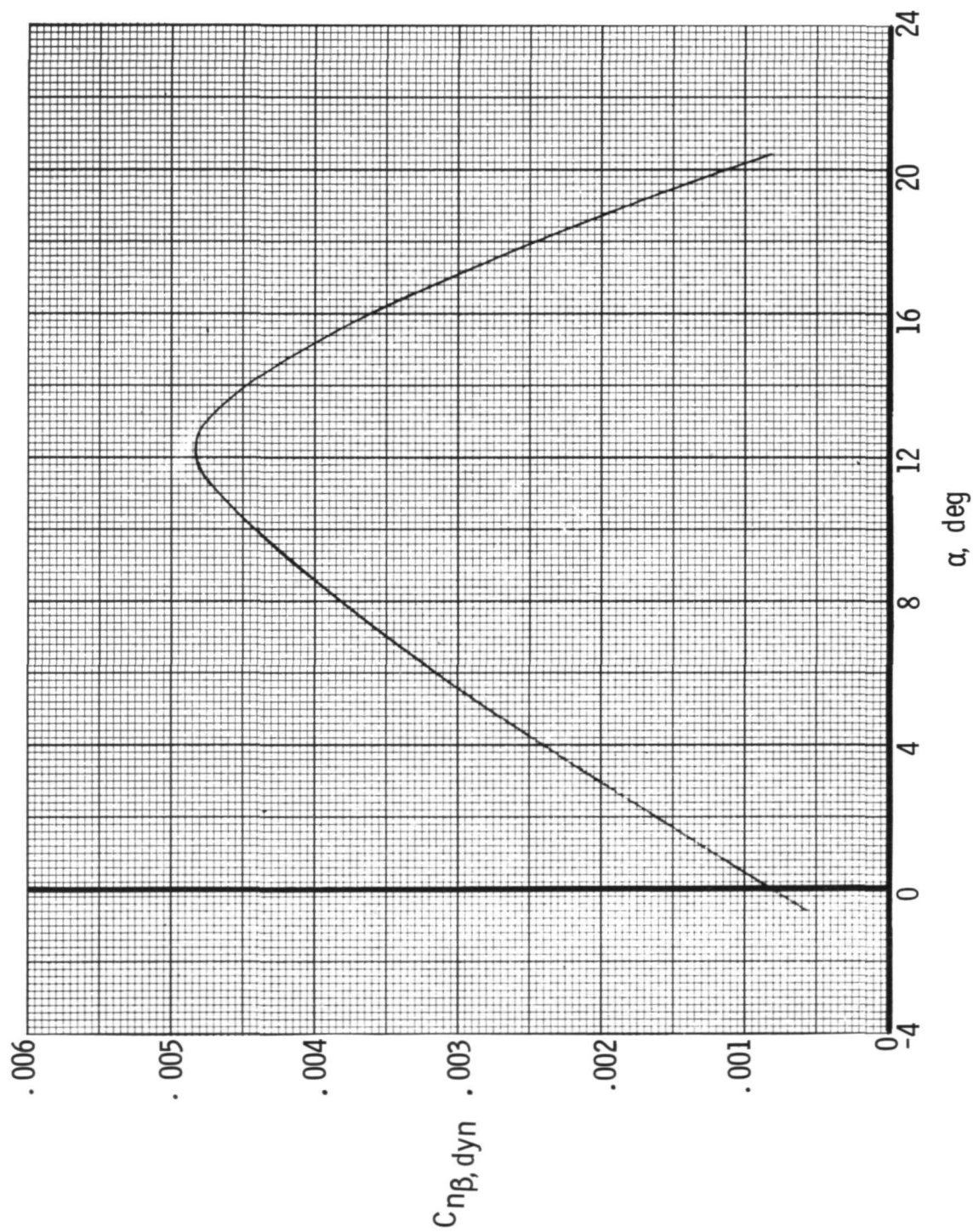


Figure 8.- Calculated values of  $C_{n\beta, \text{dyn}}$ .  $I_Z/I_X = 6.85$ ;  $R = 20.83 \times 10^6$ ; model trimmed.

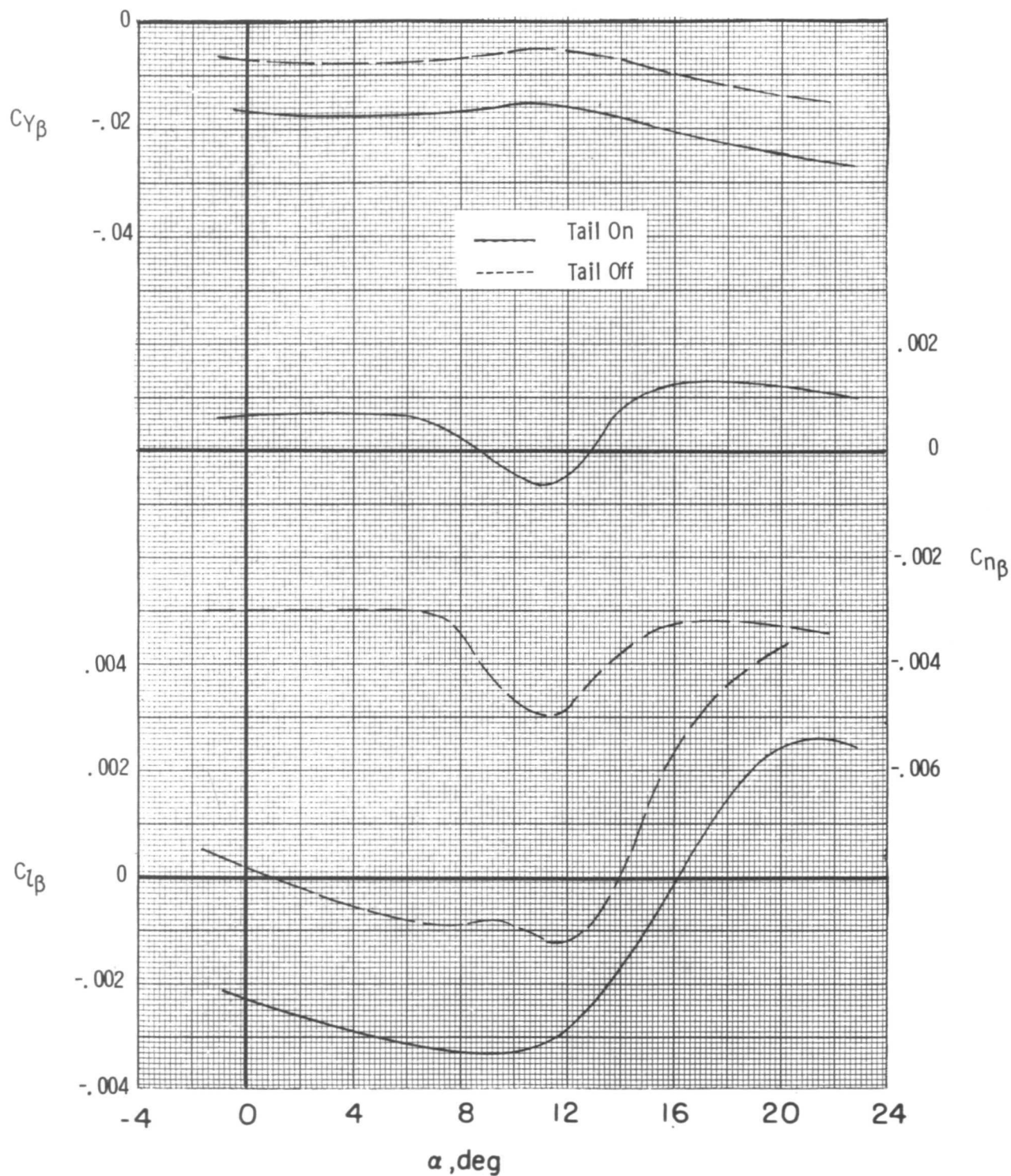


Figure 9.- Effect of vertical tail on the lateral-directional stability derivatives.  
 $R = 20.83 \times 10^6$ ;  $\delta_e = 0^\circ$ .

NATIONAL AERONAUTICS AND SPACE ADMINISTRATION  
WASHINGTON, D.C. 20546

OFFICIAL BUSINESS  
PENALTY FOR PRIVATE USE \$300

**SPECIAL FOURTH-CLASS RATE  
BOOK**

POSTAGE AND FEES PAID  
NATIONAL AERONAUTICS AND  
SPACE ADMINISTRATION  
451



POSTMASTER: If Undeliverable (Section 158,  
Postal Manual) Do Not Return

*"The aeronautical and space activities of the United States shall be conducted so as to contribute . . . to the expansion of human knowledge of phenomena in the atmosphere and space. The Administration shall provide for the widest practicable and appropriate dissemination of information concerning its activities and the results thereof."*

—NATIONAL AERONAUTICS AND SPACE ACT OF 1958

## NASA SCIENTIFIC AND TECHNICAL PUBLICATIONS

**TECHNICAL REPORTS:** Scientific and technical information considered important, complete, and a lasting contribution to existing knowledge.

**TECHNICAL NOTES:** Information less broad in scope but nevertheless of importance as a contribution to existing knowledge.

**TECHNICAL MEMORANDUMS:** Information receiving limited distribution because of preliminary data, security classification, or other reasons. Also includes conference proceedings with either limited or unlimited distribution.

**CONTRACTOR REPORTS:** Scientific and technical information generated under a NASA contract or grant and considered an important contribution to existing knowledge.

**TECHNICAL TRANSLATIONS:** Information published in a foreign language considered to merit NASA distribution in English.

**SPECIAL PUBLICATIONS:** Information derived from or of value to NASA activities. Publications include final reports of major projects, monographs, data compilations, handbooks, sourcebooks, and special bibliographies.

**TECHNOLOGY UTILIZATION PUBLICATIONS:** Information on technology used by NASA that may be of particular interest in commercial and other non-aerospace applications. Publications include Tech Briefs, Technology Utilization Reports and Technology Surveys.

*Details on the availability of these publications may be obtained from:*

**SCIENTIFIC AND TECHNICAL INFORMATION OFFICE**

**NATIONAL AERONAUTICS AND SPACE ADMINISTRATION**

**Washington, D.C. 20546**